14TH EUROPEAN CONFERENCE ON COMPOSITE MATERIALS
7-10 June 2010, Budapest, Hungary
Paper ID: 290-ECCM14

MECHANICAL AND THERMAL RESPONSE OF I-PP & S-PP/MWNT NANOCOMPOSITES

D.E. Mouzakis[1]* and I. Zuburtikudis[2]

[1] *Technological Educational Institute of Larisa, School of Mechanical Engineering, Zip 411 10, Larisa Greece, and Hellenic Army Academy, 16673, Vari, Attika, Greece*
[2] *Technological Educational Institute (TEI) of West Macedonia, Kozani, Greece*
**mouzakis@teilar.gr*

Abstract

Nanocomposites based in polypropylene (both syndiotactic and isotactic) and Multiwall Carbon Nanotubes (MWNTs) directly blended in the melt via micro-extrusion, were studied. Differential Scanning Calorimetry thermal tests and Essential Work of Fracture toughness were performed on these nanocomposites. The aim was to determine the role of MWNTs, on the creation of the plastic zone and crack propagation in double -cracked tensile specimens. Results have shown a non-linear relationship of almost all properties with MWNTs content. The thermal characterization was aimed at the evaluation of the crystallinity and the melting and crystallization temperatures of both iPP and sPP nanocomposites reinforced with MWNTs. In all cases, the effect of MWNT weight fraction on the above properties was extensively studied. MWNTs have been confirmed to influence the mobility of the polymer matrix resulting in shifts in the material melting temperature and matrix crystallinity. It was also found that a crack/craze bridging mechanism can be detected in polymer matrix/ MWNT nanocomposites. This mechanism was observed as a nano-crazing procedure, in fibrillated areas of the specimen expressed as nanotube-bridged micro-cracks. These results point a promising role of the nanotubes as tougheners for future nanocomposites applications.

1 Introduction

Nanocomposite materials are nowadays widely studied as potential high performance materials. During the past 20 years, emphasis has been given on the development of polymeric nanocomposites, where at least one of the dimensions of the filler material is sized below 100nm.

The transition from microparticles to nanoparticles provides dramatic changes in material properties. Nanoscale materials possess a large surface area for a given volume [1]. Due to the fact that many important chemical, physical and mechanical interactions (i.e load transfer capacity) are governed by surfaces and surface properties [2], a nanostructured material can exhibit substantially different properties from a micro- or macro-dimensional material of the same composition. In the case of particles and fibers, the surface area per unit volume is inversely proportional to the material's diameter, thus, the smaller the diameter, the greater the surface area per unit volume [1]. It has been shown that a change in particle diameter, layer thickness, or fiber diameter from the micrometer to nanometer scale, will affect the surface area-to-volume ratio by three orders of magnitude [3]. The increased surface to volume ratio of the reinforcing phase diversifies nanocomposites from the classic composite materials. Current research findings have shown that the use of nano-dimensioned reinforcements may lead to new materials with advanced mechanical, thermal and electrical properties [2-4]. The effective interfacial area between matrix and reinforcement is increased

compared to the respective one in classical micro-composites. As a result, the ability of load transfer from the matrix to the reinforcement [2] in the case of nanocomposites is tremendously increased. Typical nanomaterials currently under investigation include nanoparticles, nanotubes, nanofibers, fullerenes, and nanowires [4].

An attempt to study the toughness response of two polypropylene matrices reinforced with multiwall nanotubes was the aim of the present study. Purpose was to investigate the influence on the mechanical properties in DENT (double end notched) nanocomposite specimens. Two different polypropylene isomers namely isotactic polypropylene (iPP) and syndiotactic polypropylene (sPP) served as matrices and Multi Walled Carbon Nanotubes (MWNT) was used as nano-reinforcement. The MWNT's were melt mixed with the the iPP and sPP matrix. The essential work of fracture method (EWF) was applied in double-edge notched specimens in order to determine toughness. Thermal response and crystallinity of the nanocomposites was studied by differential scanning calorimetry

2 Materials and Testing

Two different kinds of MWNTs were used for the fabrication of nanocomposites: Nanotubes of ~95% purity (Nanothinx Patras, Greece), and nanotubes dispersed in an isotactic polypropylene 20% w/w master batch (Hyperion Catalysis International) respectively. Polypropylene matrices had the following characteristics:
(a). Isotactic polypropylene iPP: M_n=50000, M_w/M_n=3.8, MFI = 35.00 gr/10 min (230ºC/2.16 Kg, ASTM D 1238). iPP was melt blended with the master batch with MWNTs ending at various wt% : 0.3, 0.5, 0.75, 1, 1.5, 2, 3, 4, and 5 respectively.
(b). syndiotactic polypropylene sPP: M_n=54000, M_w/M_n=2.35, MFI = 4.50 gr/10 min (230ºC/2.16 Kg, ASTM D 1238). sPP was melt blended with MWNTs at the following wt% : 0.3, 0.5, 0.75, 1, 1.5, 3, and 5 respectively.

A ThermoHaake 'MiniLab' Micro-Compounder/Extruder was used for the preparation of both the iPP and sPP/MWNTs nanocomposites through the melt blending technique. Temperature was set at 180 ºC, rotational speed was 200 rpm, residence time of (PP and MWNTs) inside the drum was 30 min after the introduction of MWNTs in the device, in N_2 atmosphere. A home-made thermal press was employed for the compression molding of circular 100 mm disks (t~1 mm) made of the nanocomposite materials. Mold temperature was 170 ºC. The pressure would be set at 150 bar for 5 min, then it would be raised to 300 bar for additional 5 min and finally, the temperature would be decreased from 170 ºC to 40 ºC at a sufficiently low rate in order to cool the plates down to almost ambient temperature.

Deeply double edge-notched tensile (DDEN-T) specimens were cut in rectangular shape with dimensions 60x15x0.3 mm as shown in Figure 1. All tensile experiments were performed using an INSTRON 4301 testing machine at the Composite Materials Group laboratory, University of Patras, Greece. Specimens were subjected to tensile testing with a strain rate of 1mm/min. The total width of the iPP-MWNT's specimens was 15 mm and notches of lengths from 1-6 mm were created. DSC scans were performed in a Pyris Calorimeter of Perkin-Elmer. Heat-Cool rates of the nanocomposite specimens were set at 10º C/min. Each DSC scan was repeated three times and results were averaged. A LEO 35 SUPRA VP (Zeiss) field emission scanning electron microscope (FESEM) was employed for the examination of the fracture surfaces of the DDEN-T specimens.

2.1 Essential Work of Fracture

The essential work of fracture (EWF) approach is often adopted for semi-static testing analysis of the fracture toughness of many polymer systems;. The EWF protocol prescribes recording the load-displacement curve of specimens containing a single or double notch stress concentration zone designed to provoke a fully yielded (if possible) plastic zone in the fracture plane. From the integral of that curve, it is possible to calculate the total work required to produce this yielded fracture region, W_f, which can be expressed as a function of the EWF, W_e, and the non-EWF, W_p:

$$W_f = W_e + W_p = w_e l t + \beta w_p l^2 t \qquad (1)$$

where w_e and w_p are the specific values for W_e and W_p, l and t are the ligament length and thickness of the fracture specimen, and β is a shape factor associated with the dimension of the plastic zone normal to the crack plane. Thus, by normalizing Equation 1, the specific total work of fracture, wt, is expressed a linear function of l, the ligament length:

$$w_f = w_e + \beta w_p l \qquad (2)$$

from which the value of EWF, w_e, is given by its y-axis intercept and the value of non-EWF, w_p, is proportional to its slope. Theory, experimental procedures and validation for the EWF approach is well described in numerous publications [5,6,7] as well as the equivalent nature of the specific essential work of fracture (w_e) parameter to the J-Integral (J_{IC}) and plain stress fracture toughness (G_{IC}) for ductile polymers and composites. It has been also applied for the toughness evaluation of polyolefin matrix nanocomposites with interesting results for both static [8-9] and impact testing [10] procedures.

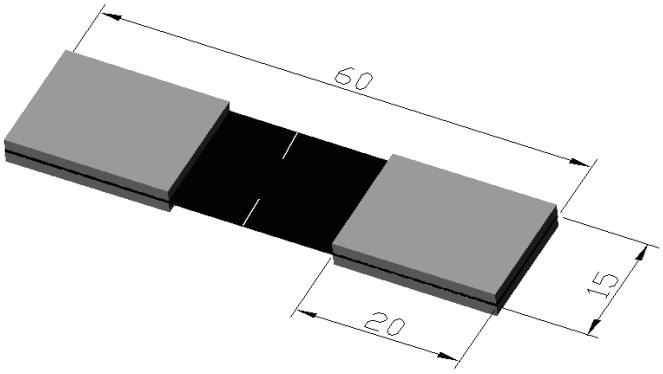

Figure 1. Typical Dimensions of iPP-sPP/MWNT's, DDEN-T specimens

3 Results and Discussion

3.1 Differential Scanning Calorimetry

The complex thermal character of the sPP matrix and its nanocomposites can be evidenced from Figure 3. sPP is well known for its crystal polymorphism which has already been extensively studied with and without loading [11-13]. For all specimens a partial melting of the trans-planer form III around 65 ºC can be seen, which was suppressed for the 5wt% in MWNT specimens. Moreover, a double melting peak is present for pure sPP; around 130 ºC is the melting point of the stable helical form I, and at ca. 120 ºC melting of the disordered

form I takes place [13]. This disordered form I is suppressed by the existence of MWNT which favor the helical form I crystals as proven by the graphs in Figure 3. In fact, it has been found, that nanoparticles, in general, favor this type of crystallization in sPP matrices [14]. On the other hand, iPP matrix behaves in a much more conformal way during melting and the only profoundly visible feature is the shifting in the nanocomposites' T_m with increasing nanotube content as shown in Figure 2.

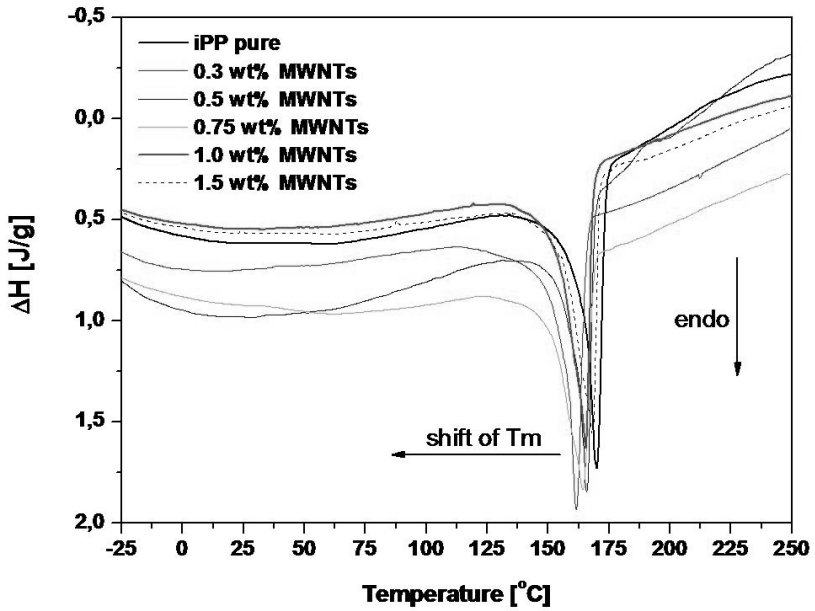

Figure 2. Indicative DSC heat scans for the iPP/MWNT nanocomposites

Results obtained from the DSC thermal scans are shown in Tables 1 and 2 for the iPP and sPP nanocomposites respectively. Melting peak was determined from the main melting peak maximum, melt and crystallization enthalpies were calculated by the melt and crystallization peak integrals, respectively. Crystallinity (%) was calculated by reducing the melt and crystallization enthalpies to the corresponding heats of fusion for iPP (209 J/g) and sPP (196 J/g) [15].

iPP +%wt in MWNT	*Melting Peak* (ºC)	*Crystallization Peak* (ºC)	*Melt Enthalpy (J/g)*	*Crystallization Enthalpy (J/g)*	*Crystallinity (%)*	*Crystallinity (cooling) (%)*
pure	167.1	112.1	15.7	18.9	7.5	9.0
0.3	164.4	124.9	20.1	14.1	9.6	6.7
0.5	164.8	126.3	12.4	12.0	5.9	5.8
0.75	164.0	126.1	14.0	13.4	6.7	6.4
1.0	164.5	126.7	12.0	13.2	5.7	6.3
1.5	166.9	128.5	19.5	12.7	9.3	6.1
5.0	169.2	132.2	8.8	10.7	4.2	5.1

Table 1. iPP/MWNT nanocomposites DSC results

As far as iPP matrix is concerned, it can be deduced from Table 1 that for MWNT nanocomposites melt temperature is lowered by 2-3 degrees (with an exception for 5wt%). This implies that MWNT's act as nuclei for earlier crystallization. However, the corresponding crystallization peak temperatures during cooling are increasing with increasing MWNT content, which points to the direction of higher order crystal packing. Overall crystallinity data, however, do not confirm higher amounts of crystalline content for the iPP

matrix in these nanocomposites. With an exception for 0.3 and 1.5 wt% in MWNT the overall crystallinity is lower than that of pure iPP. This is also the picture delivered by crystallization data during the cooling phase as seen in Table 1.

Generally, sPP matrix exhibited an increasing T_m effect with increasing MWNT content. This was also the case for the crystallization peak temperature T_c, during cooling. These effects imply higher order molecular orientation and packing expressed by the increasing helical form I accompanied by decreasing trans-planar form III and the vanishing of disordered form I, as evidenced by Figure 3. The overall crystalline content does not vary a lot with increasing MWNT content, as seen in Table 3. One can observe that crystallinity rises up to 1 wt% in MWNT's and lowers for higher MWNT contents. The same picture more or less is valid for the crystallinity variations during the cooling phase.

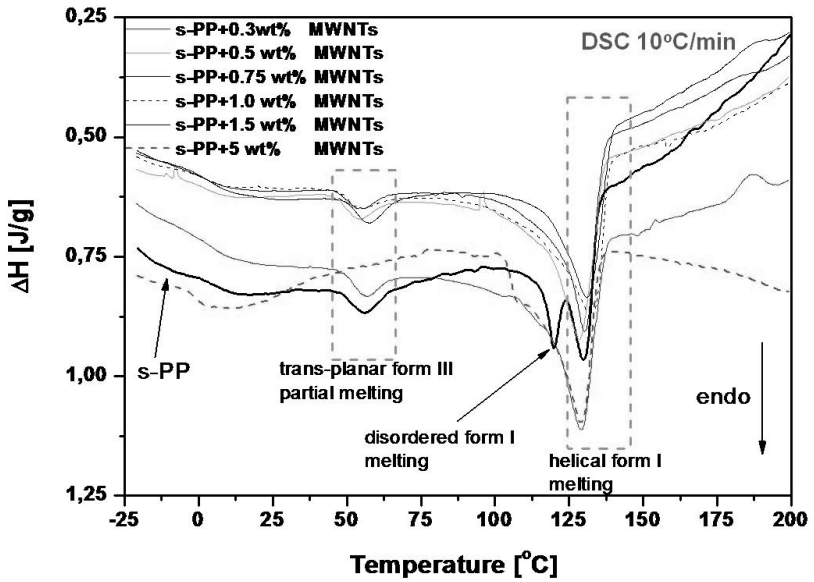

Figure 3. Indicative DSC heat scans for the sPP/MWNT nanocomposites

sPP +%wt in MWNT	*Melting Peak* (ºC)	*Crystallization Peak* (ºC)	*Melt Enthalpy (J/g)*	*Crystallization Enthalpy (J/g)*	*Crystallinity (melting) (%)*	*Crystallinity (cooling) (%)*
pure	125.8	72.0	3.9	5.2	2.0	2.7
0.3	128.2	91.6	5.1	3.8	2.6	2.0
0.5	126.6	95.5	5.6	3.9	2.9	2.0
0.75	130.7	96.7	6.5	3.5	3.3	1.8
1.0	130.3	98.0	5.9	3.2	3.0	1.6
1.5	129.8	99.6	2.1	1.8	1.1	0.9
3.0	133.0	102.7	3.4	1.6	1.7	0.8
5.0	131.0	137.3	3.3	5.2	1.7	2.7

Table 2. sPP/MWNT nanocomposites DSC results

3.2 Essential Work of Fracture Toughness

A somewhat brittle behaviour was witnessed for most of the iPP/MWNT nanocomposite DDEN-T specimens at all nanotube wt% contents. It is well known that iPP exhibits high notch sensitivity [16], and this behaviour was not improved by the addition of the nanotubes as seen in Figure 4. The force elongation curve shows that after an elastoplastic region near

load maximum the specimen fails abruptly, showing no stable crack propagation phase. Quite on the contrary, sPP/MWNT nanocomposites showed the ideal necking-yielding-stable neck tearing sequence which is usually desired for the application of the EWF approach in DDEN-T specimens [5,6]. Load increases until a sudden drop marks ligament yielding, followed by a stable tearing phase of the yielded ligament as seen in Figure 5.

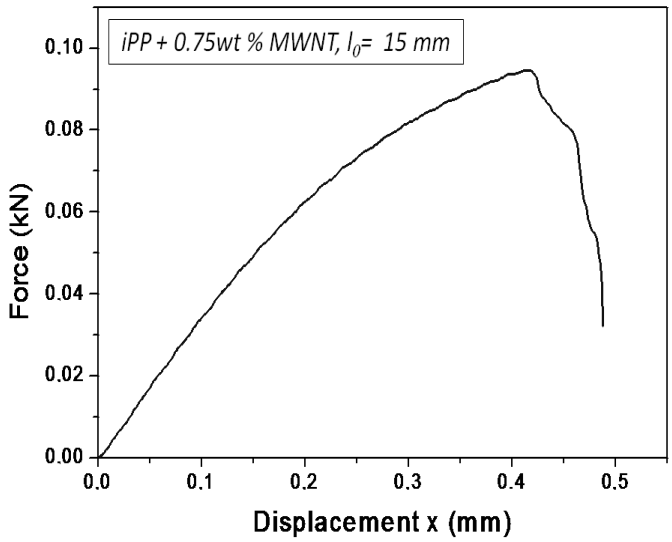

Figure 4. Typical DDEN-T specimen force-displacement curve at 1mm/min, for the iPP/0.5wt%MWNT nanocomposite DDEN-T specimens

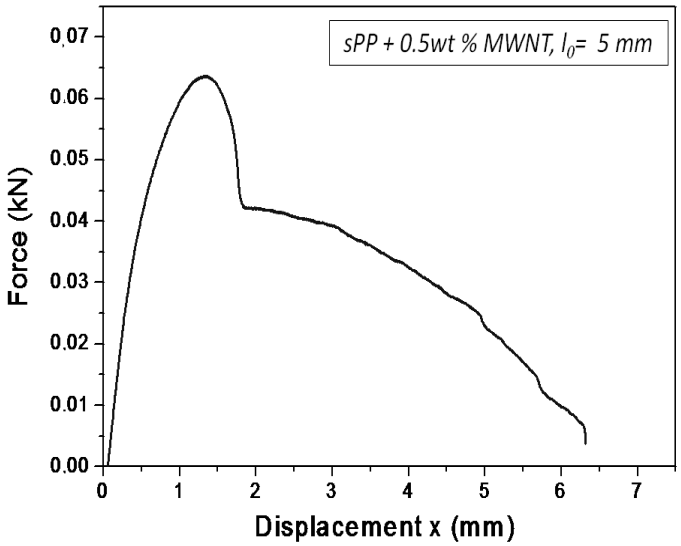

Figure 5. Typical DDEN-T specimen force-displacement curve at 1mm/min, for the sPP/0.75wt% MWNT nanocomposite DDEN-T specimens

The specific work of fracture (w_f) vs ligament size plots for the iPP/MWNT and sPP/MWNT nanocomposites are presented in Figures 6 and 7 respectively. Both nanocomposite categories, exhibited relatively unstable behaviour with increasing ligament size as witnessed by observing these graphs. It is probably the effect of relatively inadequate dispersion of the nanotubes in the iPP and sPP matrices accountable for this behaviour.

As mentioned in the related literature [17-19] carbon nanotube (CNT) nanocomposites exhibit their highest mechanical performance at nanotube concentrations within the range of 0.3%

and 1-2% by weight. There exist however, works stating that CNT nanocomposites deliver best results at concentrations around of 3 wt% [20]. Bar diagram shown in Fig.8, proves that the results of the present work agree well with respective data presented in literature. The maximum essential work of fracture toughness (w_e) was recorded for the iPP/0.75wt% MWNT nanocomposites accompanied by a relative good increase in yield stress for these specimens with respect to pure iPP. Other concentrations from 1.5 to 3wt% in MWNT delivered second best toughness and yield stress data. So the best possible toughness/yield strength is to be achieved for MWNT contents ranging from 0.75 – 3wt% with the exception of 1wt%, probably owing to bad dispersion of MWTs. Nanocomposites below 0.75 wt% and above 4wt% in MWNT's delivered results similar to the pure iPP matrix, owing either to very low or too high (large agglomerates) CNT content in order to produce efficient results.

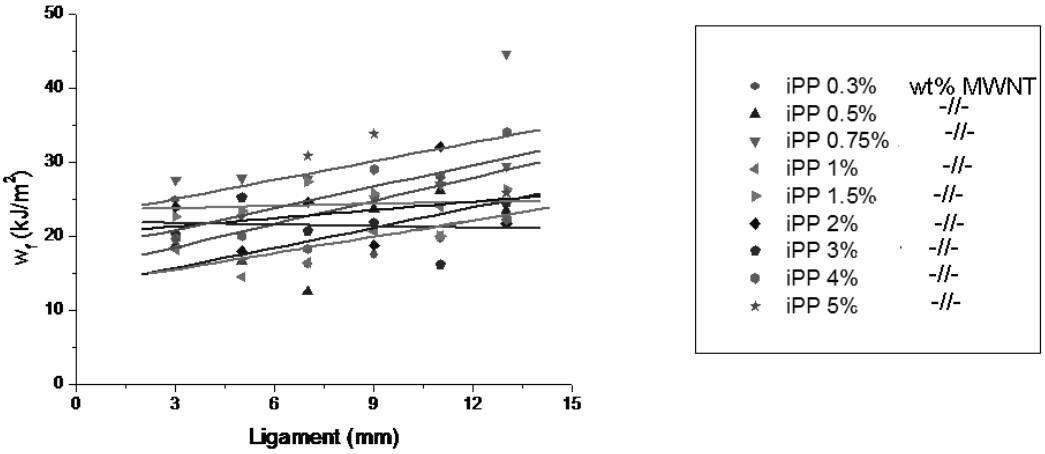

Figure 6. Specific work of fracture against ligament size for the iPP/MWNT DDEN-T specimens

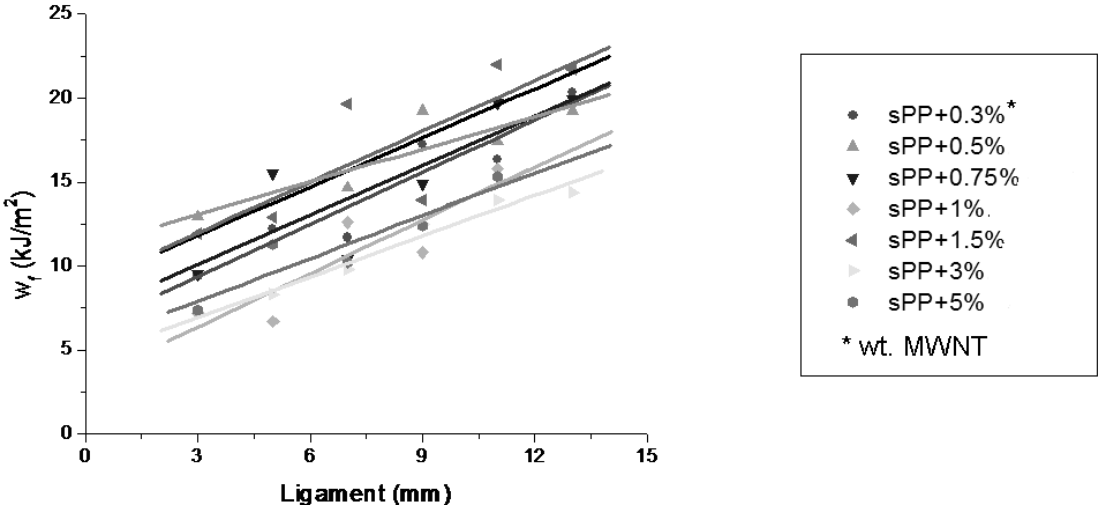

Figure7. Specific work of fracture against ligament size for the sPP/MWNT DDEN-T specimens

The composite bar chart shown in Fig. 9 presents the EWF–toughness and yield stresses for the sPP/MWNT nanocomposites. The behavior of these systems was also according to similar studies. There appears to be an optimum in toughness/yield stress ratio for MWNT concentrations around 0.5wt%. Again, 1wt% did not respond efficiently enough and compositions between 1.5 and 3wt% in MWNT's delivered second best data. Above 3wt%

and below 0.5wt% the nanotubes either do not disperse very well or are not enough to produce a reinforcing effect.

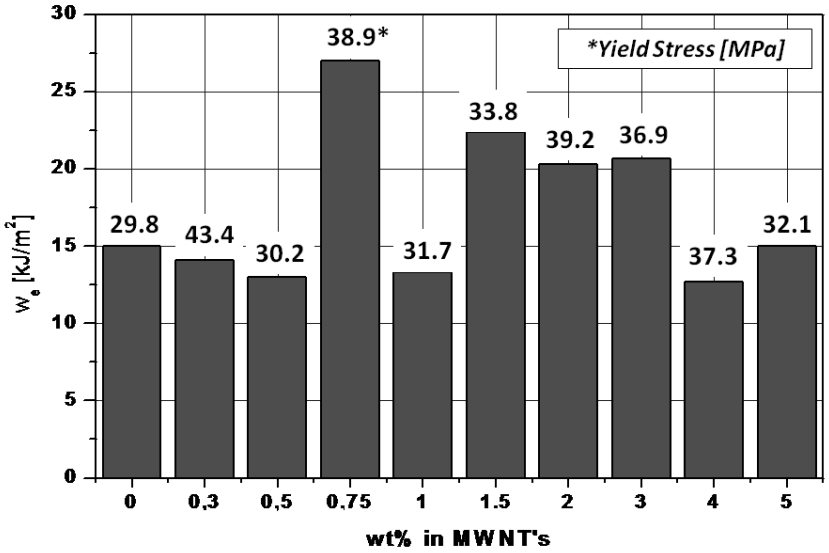

Figure 8. Bar Chart presenting EWF toughness and DDENT-T yield stress (*) for iPP/MWNT nanocomposites.

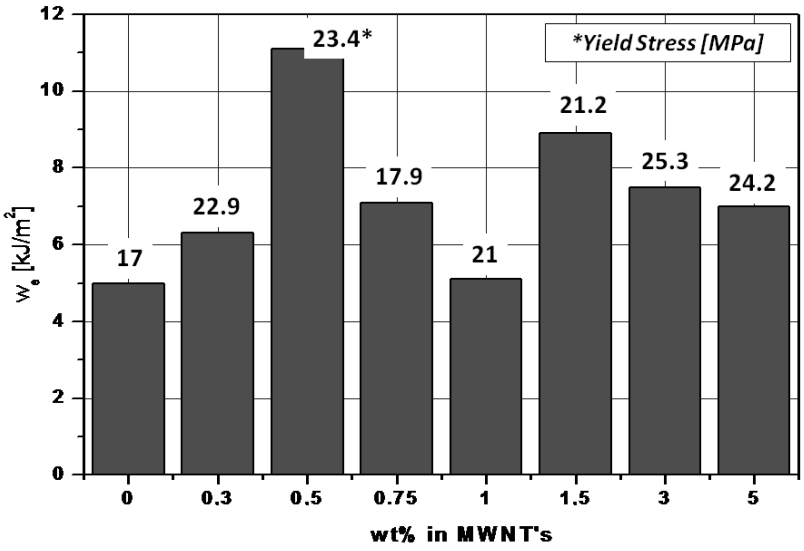

Figure 9. Bar Chart presenting EWF toughness and DDENT-T yield stress (*) for sPP/MWNT nanocomposites.

3.3 Scanning Electron Microscopy (SEM)

Scanning Electron photomicrographs were taken for the DDEN-T specimen concentrations which delivered the best EWF toughness/yield stress results. It is observed that in the case of the iPP-matrix nanocomposite a better dispersion of particles is achieved compared to respective nanotubes dispersion in sPP-matrix materials.
Figure 10A shows a ductile micro-fibrillated area, typical for stress-whitened yielded areas of a polymer. Further examination of that area in higher magnifications however showed interesting features as seen in Figure 10B. Closer examination of the polymer micro fibrils revealed crazes (framed area) running around the bases of the fibrils. These crazes (inset view) are bridged by multiwall nanotubes of about 50 nm diameter. So, crazing and nanotube-supported craze or crack bridging effects are discovered for this type of nanocomposites as

energy dissipation mechanisms corroborative to the matrix fibrillation. In fact, as early as back in 2000 it was already stated that CNT's can bridge the cleavages of micro-cracks [21-22]. CNT's exhibited this effect in acrylic matrices reinforced with single [21], or multiwall CNT's [23] resulting in improved toughness and strength. Fatigue resistance of epoxy matrices has also been reported to impove by CNT-crack bridging mechanisms [24, 25] for the same reason. In fact, even ceramic hybric composites have been reported to owe increased toughness to the same mechanism [26].

In Figure 11, a nanotube aggregate (Figure 11A) is presented. The existence of such aggregates is mainly responsible for the low mechanical properties observed in sPP-matrix nanocomposites, since they act as flaws within the material, decreasing the overall interfacial area available. At higher magnifications (Figure 11B) nanofibrills probably composed of both sPP and MWNT's can be seen. So, the main energy dissipation mechanisms for the sPP/MWNT nanocomposites are matrix nanofibrillation (Figure 11B) and ductile polymer macro-tearing as seen in Figure 11A.

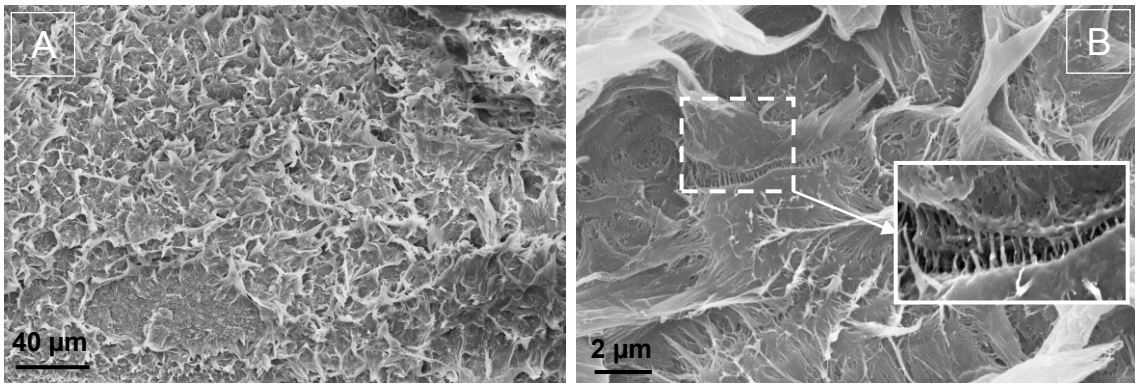

Figure 10. SEM photomicrographs for iPP/MWNT's (0.75 wt% MWNT). A. Fibrillated area, B. Maginification of area A with inset view showing a microcrack bridged by MWNT's

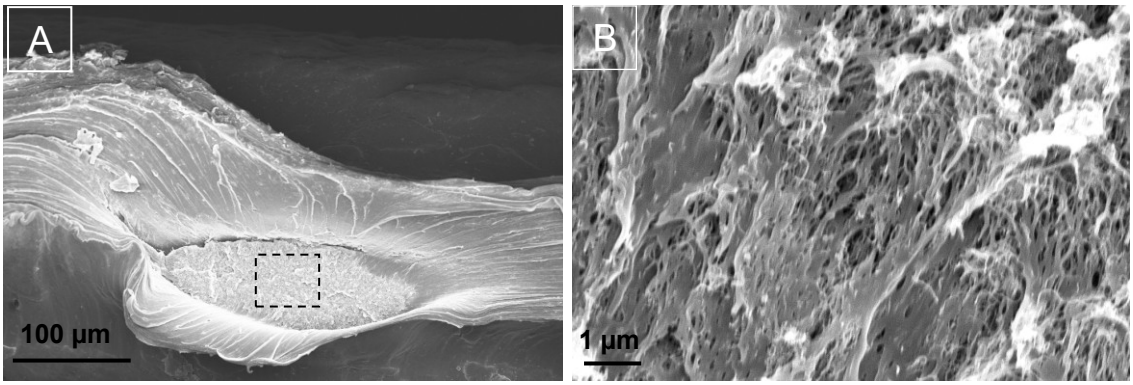

Figure 11. SEM photomicrographs for sPP/MWNT's (0.5 wt% MWNT). A. Ductile tearing with a MWNT agglomerate, B. Detail of framed area in the large agglomerate

4 Conclusions

In the present paper the mechanical properties of two different types of CNT polyolefin matrix nanocomposites were investigated. Namely; iPP/MWNT and sPP/MWNT nanocomposites. In the case of carbon nanotubes nanocomposites, the effect of both the notch length and the concentration in carbon nanotubes on the overall behaviour was studied by

means of the EWF toughness. Also DSC experiments delivered the matrix crystallinity and shifts in the melting and crystallization temperature due to the presence of MWNTs. Experimental results have shown that a superior mechanical performance was observed in general for nanotube concentrations between 0.5-0.75wt% as well as in the region 1.5-3% for both matrix systems. The presence of MWNTs in the polymer matrices did not enhance the overall crystallinity, but showed indications for facilitating higher order molecular packing especially in the case of sPP. Finally, crack bridging in the nanoscale was confirmed in the case of iPP/MWNTs as a secondary toughening mechanism corroborating matrix yielding and fibrillation.

Acknowledgement
The authors are thankful to the Composite Materials Group laboratory, University of Patras, for providing kind help and support during experimental procedures.

References

[1] Luo J. J., and Daniel I. M.: Characterization and Modeling of Mechanical Behavior of Polymer/Clay Nanocomposites. Composites Science and Technology, 63(11), 1607–1616 (2003). DOI:10.1016/S0266-3538(03)00060-5
[2] Jose M. V., Dean D., Tyner J., Price G., Nyairo E.: Polypropylene/carbon nanotube nanocomposite fibers: Process-morphology- property relationships. Journal of Applied Polymer Science 103(6), 3844-3850 (2007). DOI:10.1002/app.25475
[3] Thostenson E., Li C., and Chou T.: Review Nanocomposites in Context, Journal of Composites Science & Technology, 65, 491–516 (2005). DOI:10.1016/j.compscitech.2004.11.003
[4] Hussain F., Hojjati M., Okamoto M. and Gorga R. E.: Review Polymer-matrix Nanocomposites, Processing, Manufacturing, and Application: An Overview Journal of Composite Materials 40, 1511-1575 (2006). DOI: 10.1177/0021998306067321
[5] Mouzakis D. E.: Application of the Essential Work of Fracture Method for Ductile Polymer Systems, Mensch & Buch Verlag, Berlin, (1999).
[6] Karger-Kocsis J.: in 'Fracture of Polymers, Composites and Adhesives' (eds.: Williams J.G. and Pavan A.), ESIS Publication 27, Elsevier Science, Oxford, 213-230 (2000).
[7] Clutton E.: in 'Fracture Mechanics Testing Methods for Polymers, Adhesives and Composites', (eds.: Moore D. R., Pavan A., and Williams J.G.), ESIS 28, Elsevier Science, Oxford, 177-195 (2001).
[8] Bureau M.N., Perrin-Sarazin F., and Ton-That M.-T.: Polyolefin Nanocomposites: Essential Work of Fracture Analysis. Polymer Engineering and Science, 44(6), 1142-1151 (2004). DOI: 10.1002/pen.20107
[9] Mouzakis D.E., Papanicolaou G.C., Argyrakis Chr., Kandilioti G., Kontarinis D. and Gregoriou V.G.: Fracture Toughness Response and Residual Property Modelling in Polymer Nanocomposites. Journal Nanostructured Polymers and Nanocomposites, 4, 100-109 (2008).
[10] Bao S.P., Tjong S.C.: Impact essential work of fracture of polypropylene/montmorillonite nanocomposites toughened with SEBS-g-MA elastomer. Composites: Part A 38, 378–387 (2007). DOI:10.1016/j.compositesa.2006.03.005
[11] Gregoriou V. G., Kandilioti G., Gatos K. G.: An infrared spectroscopic approach to the polymorphic behavior of syndiotactic polypropylene and its crystal-crystal transformation during mechanical stretching. Vibrational Spectroscopy, 34, 47–53 (2004). DOI: 10.1016/j.vibspec.2003.08.004\
[12] Ebener H., Pleuger B., Petermann J.: Stress and strain oscillations in syndiotactic polypropylene and in poly(ethylene terephthalate). Journal of Applied Polymer Science, 71, 813–817 (1999). DOI: 10.1002/(SICI)1097-4628(19990131)71:5<813::AID-APP15>3.0.CO;2-P

[13] Gatos K.G., Kandilioti G., Galiotis C., Gregoriou V.G.: Mechanically and thermally induced chain conformational transformations between helical form I and trans-planar form III in syndiotactic polypropylene using FT-IR and Raman spectroscopic techniques. Polymer, 45, 4453–4464 (2004). DOI: 10.1016/j.polymer.2004.03.095

[14] Mouzakis D.E.: Study of the stress oscillation phenomenon in syndiotactic polypropylene/montmorillonite nanocomposites. Express Polymer Letters 4, 244–251 (2010). DOI: 10.3144/expresspolymlett.2010.31

[15] Zhang X., Zhao Y., Wang Z., , Zheng C., Dong X., Su Z., Sun P., Wang D., Han C.C., Xu D.: Morphology and mechanical behavior of isotactic polypropylene (iPP)/syndiotactic polypropylene (sPP) blends and fibers. Polymer 46, 5956–5965 (2005). DOI:10.1016/j.polymer.2005.05.004

[16] Mouzakis D.E., Striker F., Mühlhaupt R., and Karger-Kocsis J.: Fracture Behaviour of Polypropylene/Glass Bead/ Elastomer Composites by Using the Essential Work of Fracture Method. Journal of Materials Science 33, 2551-2562 (1998). DOI:10.1023/A:1004345017105

[17] Zhou Y., Pervin F., Lewis L., Jeelani S.: Experimental study on the thermal and mechanical properties of multi-walled carbon nanotube-reinforced epoxy, Materials Science and Engineering A, 452-453, 657-664 (2007). DOI:10.1016/j.msea.2006.11.066

[18] Kim J.Y., Park H.S., Kim S.H.: Multiwall-carbon-nanotube-reinforced poly(ethylene terephthalate) nanocomposites by melt compounding. Journal of Applied Polymer Science, 103(3), 1450-1457 (2007). DOI:10.1002/app.25377

[19] Xiao Y., Zhang X., Cao W., Wang K., Tan H., Zhang Q., Du R., Fu Q.: Dispersion and mechanical properties of polypropylene/multiwall carbon nanotubes composites obtained via dynamic packing injection molding. Journal of Applied Polymer Science 104 (3), 1880-1886 (2007). DOI:10.1002/app.25852

[20] Sahoo N.G., Jung Y. C., Yoo H.J., Cho J. W.: Influence of carbon nanotubes and polypyrrole on the thermal, mechanical and electroactive shape-memory properties of polyurethane nanocomposites. Composites Science and Technology 67(9), 1920-1929 (2007). DOI:10.1016/j.compscitech.2006.10.013

[21] Ajayan P. M., Schadler L.S., Giannaris C., and Rubio A.: Single-Walled Carbon Nanotube-Polymer Composites: Strength and Weakness. Advanced Materials 12(10), 750-753 (2000). DOI 0935-9648/00/1005-0751

[22] Qian D., Dickey E.C., Andrews R. and T. Rantell.: Load transfer and deformation mechanisms in carbon nanotube-polystyrene composites. Applied Physics Letters 76(20), 2868-2870 (2000). DOI: 10.1063/1.126500

[23] Mathur R.B., Pande S., Singh B.P., Dhami T.L.: Electrical and mechanical properties of multi-walled carbon nanotubes reinforced PMMA and PS composites. Polymer Composites 29(7), 717-727 (2008). DOI: 10.1002/pc.20449

[24] Zhang W., Picu R.C. and Koratkar N.: The effect of carbon nanotube dimensions and dispersion on the fatigue behavior of epoxy nanocomposites. Nanotechnology 19, 1-5 (2008). DOI:10.1088/0957-4484/19/28/285709

[25] Zhang W., Srivastava I., Zhu Y.-F., Picu C.R., and Koratkar N.A.: Heterogeneity in Epoxy Nanocomposites Initiates Crazing: Significant Improvements in Fatigue Resistance and Toughening. Small 5(12), 1403–1407 (2009). DOI: 10.1002/smll.200801910

[26] Ahmad K., Pan W.: Hybrid nanocomposites: A new route towards tougher alumina ceramics. Composites Science and Technology 68, 1321–1327 (2008) DOI:10.1016/j.compscitech.2007.12.011